

Article

Constituents from *Ageratina pichinchensis* and Their Inhibitory Effect on Nitric Oxide Production

Mariana Sánchez-Ramos ¹, Araceli Guerrero-Alonso ², Antonio Romero-Estrada ³, Judith González-Christen ⁴,
Laura Alvarez ², Juan José Acevedo-Fernández ⁵, Angélica Román-Guerrero ¹, Francisco Cruz-Sosa ^{1,*}
and Silvia Marquina-Bahena ^{2,*}

¹ Department of Biotechnology Autonomous Metropolitan, University-Iztapalapa Campus, Av. Ferrocarril de San Rafael Atlixco 186, Col. Leyes de Reforma 1^a, Sección, Alcaldía Iztapalapa, México City 09310, CDMX, Mexico; marianas_ramos_06@xanum.uam.mx (M.S.-R.); arogue@xanum.uam.mx (A.R.-G.)

² Chemical Research Center-IICBA, Autonomous University of the State of Morelos, Av. Universidad 1001, Chamilpa, Cuernavaca 62209, Morelos, Mexico; araceli.guerrero@uaem.edu.mx (A.G.-A.); lalvarez@uaem.mx (L.A.)

³ Department of Wood, Pulp and Paper, University Center of Exact Sciences and Engineering, University of Guadalajara, Km. 15.5, Guadalajara-Nogales, Col. Las Agujas, Zapopan 45200, Jalisco, Mexico; antonio.romero@academicos.udg.mx

⁴ Faculty of Pharmacy, Autonomous University of the State of Morelos, Av. Universidad 1001, Chamilpa, Cuernavaca 62209, Morelos, Mexico; judith.gonzalez@uaem.mx

⁵ Faculty of Medicine, Autonomous University of the State of Morelos, Leñeros s/n, Col. Los Volcanes, Cuernavaca 62359, Morelos, Mexico; juan.acevedo@uaem.mx

* Correspondence: cuhp@xanum.uam.mx (F.C.-S.); smarquina@uaem.mx (S.M.-B.)



Citation: Sánchez-Ramos, M.; Guerrero-Alonso, A.; Romero-Estrada, A.; González-Christen, J.; Alvarez, L.; Acevedo-Fernández, J.J.; Román-Guerrero, A.; Cruz-Sosa, F.; Marquina-Bahena, S. Constituents from *Ageratina pichinchensis* and Their Inhibitory Effect on Nitric Oxide Production. *Appl. Sci.* **2024**, *14*, 3942. <https://doi.org/10.3390/app14093942>

Academic Editor: Burkhard Poeggeler

Received: 18 March 2024

Revised: 30 April 2024

Accepted: 3 May 2024

Published: 6 May 2024



Copyright: © 2024 by the authors. Licensee MDPI, Basel, Switzerland. This article is an open access article distributed under the terms and conditions of the Creative Commons Attribution (CC BY) license (<https://creativecommons.org/licenses/by/4.0/>).

Abstract: In this study, we report on the isolation, purification, and anti-inflammatory evaluation of compounds from the plant species *Ageratina pichinchensis*. Using open-column chromatography, 11 known compounds were purified, which chemical structures were elucidated by nuclear magnetic resonance techniques (1D and 2D). All compounds were evaluated in an in vitro model of RAW 264.7 mouse macrophage cells, measuring the nitric oxide inhibition to determine the anti-inflammatory effect. The compound betuletol 3-O- β -glucoside (**11**) inhibited nitric oxide with a half-maximal inhibitory concentration (IC₅₀) of $75.08 \pm 3.07\%$ at 75 μ M; additionally, it inhibited the secretion of interleukin 6 (IL-6) and activation of the nuclear factor (NF- κ B). These results suggest that the anti-inflammatory effect attributed to *A. pichinchensis* species is promoted by compound **11**, which could be considered a potential anti-inflammatory agent by suppressing the expression of NF- κ B target genes, such as those involved in the proinflammatory pathway and inducible nitric oxide synthase (iNOS).

Keywords: betuletol 3-O- β -glucoside; *A. pichinchensis*; anti-inflammatory activity

1. Introduction

The plant species *A. pichinchensis* (Kunth) R.M. King & Ho. Steal. (Asteraceae) is native to Mexico and grows in 28 of its 32 states. This species is also identified by the synonyms *Eupatorium aschbornianum*, *Eupatorium pichinchense*, and *Ageratina aschenborniana* [1–3]. Particularly, in the state of Morelos, it is popularly known as “axihuitl”, and it is used in traditional medicine for treating stomach pain, respiratory issues, gastrointestinal problems, and skin infections [4,5].

Scientific studies carried out using different biological evaluation models reveal that the aerial parts of *A. pichinchensis* exhibit activity against onychomycosis and tinea pedis, gastroprotective and healing effects, and may even inhibit the in vitro proliferation of keratinocytes [6–11]. The main compounds associated with this type of biological effect are

chromenes, furans, terpenes, essential oils, and glycosylated flavonoids [8–13]. However, the anti-inflammatory effect of this plant species has not been reported.

Inflammation, a response of the immune system which stimulation can be caused by infections or stress, is associated with multiple diseases and triggers numerous biochemical, immunological, and cellular reactions [14,15]. During the inflammatory process, mediating substances that generate pain are released into the nervous system. Among these are interleukins that induce the expression of genes that encode enzymes and other chemical species that contribute to the inflammatory response [16–18].

In particular, the enzyme nitric oxide synthase (iNOS) catalyzes the formation of the free radical nitric oxide (NO) in a gaseous state that stimulates vasodilation and cannot be stored [18–21]. Notably, at low concentrations, NO plays a mediating and protective role, acting as an immunoregulatory and antimicrobial agent due to its ability to generate DNA damage, inhibit enzymes of energy metabolism and oxidize proteins, and peroxidize the membrane lipids of pathogens [19–21]. However, high concentrations of NO can damage tissues by causing iNOS overexpression and cytotoxicity, which manifests itself in acute and chronic pathological responses mediated by cytokines and endotoxins of various cell types, mainly macrophages [22–24].

The iNOS enzyme can be elicited in different cell types, such as macrophages, hepatocytes, neutrophils, etc., generating a large amount of NO that can be toxic, which is why NO functions as a proinflammatory molecule [24–26]. In the chronic phase of inflammation, the inflammatory signal can be magnified by the production of molecules, such as nuclear transcription factor kappa β (NF- κ), TNF- α , and interferon-gamma (IFN- γ), which promote the transcription of iNOS and increase vasodilation, edema, and plasma exudation [26–29]. A high production of NO can be associated with the development of diseases, such as Alzheimer's, cardiovascular, rheumatoid arthritis, pulmonary fibrosis, diabetes, and cancer, among others [27–29]. This is why the iNOS enzyme is essential in the inflammatory process and allows us to understand the mechanism of action of active ingredients from medicinal plants [30,31].

This study reports the anti-inflammatory activity of chemical compounds isolated from the aerial parts (leaves and flowers) of *A. pichinchensis* with respect to the inhibition of NO in RAW 264.7 mouse macrophage cells induced with lipopolysaccharides (LPSs).

2. Materials and Methods

2.1. General Procedures

Compounds 1–11 were characterized using spectroscopic techniques and mass spectrometry. For compounds 1, 3, 4, 6, 7, and 8, Varian Unity Inova 200 MHz equipment was used. Compounds 2, 5, 9, and 10 were analyzed using a Varian Mercury Plus 400 MHz—ID3 spectrometer (Varian Inc., Palo Alto, CA, USA). For these compounds (1–10), CDCl₃ was used, while compound 11 was dissolved in DMSO-d₆, and the spectra of ¹H, ¹³C, DEPT, COSY, HSQC, and HMBC were obtained on a Bruker AVANCE III HD 500 MHz Spectrometer (Billerica, Middlesex, MA, USA). FABMS spectra were obtained using a JEOL-AX 505HA mass spectrometer. Optical rotation was measured in CHCl₃ on a Perkin Elmer 241 digital polarimeter at 25 °C. Melting points were determined using a Prendo apparatus [32–34].

Compounds 1–11 were purified using column chromatography (CC), silica gel 60 (70–230 and 230–400 mesh) as the stationary phase and thin-layer chromatography (silica gel 60 F₂₅₄, Merck) to monitor the separation of the compounds, which were visualized using a solution of Ce(SO₄)₂ (NH₄)₂SO₄ * 2H₂O.

2.2. Plant Material

A. pichinchensis was collected in the town of San Juan Tlacotenco, municipality of Tepoztlán, Morelos, Mexico, in April 2018 (19°00'43.88" N, 99.05'38.66" W). The plant was prepared (pressed) and taken to the HUMO Herbarium of the Autonomous University of the State of Morelos (UAEM); the Biol. Gabriel Flores Franco identified this species, which is registered with voucher number 33913 [34].

2.2.1. Purification and Identification of Compounds from *A. pichinchensis* Leaves

The dry stems and leaves of *A. pichinchensis* were separately extracted three times with ethyl acetate (EtOAc) by sonication; each extraction lasted 30 min. The solvent was concentrated in a rotatory evaporator under reduced pressure. The plant material was subjected to a second extraction with the solvent methanol following the same procedure as that used for ethyl acetate. An ethanol/H₂O (95:05) extract of the flowers was obtained under the same conditions.

Leaves were selected from the collected plants and dried at room temperature. This material (1.085 kg) was extracted with EtOAc three times (each time with 4 L of the solvent).

The EtOAc extracts obtained were concentrated to dryness by distillation under reduced pressure using a rotary evaporator, obtaining 20.3 g of residue. Fractionation of the EtOAc extract by open CC (silica gel, 70–230 mesh; 10 cm i.d. × 60 cm) was performed with a gradient system of *n*-hexane/EtOAc 80:20 to 0:100, collecting 35 fractions of 300 mL.

The fractions were grouped according to their chemical profile into four groups: AP-1A (fractions 1–5, *n*-hexane: EtOAc 80:20, 4.12 g), AP-1B (fractions 6–19, *n*-hexane: EtOAc 60:40 and 40:60, 5.23 g), AP-1C (fractions 20–32, *n*-hexane: EtOAc 20:80, 5.94 g), and AP-1D (fractions 33–35, EtOAc 100%, 3.52 g).

AP-1A contains aliphatic esters, fatty acids, and *O*-methylenecalinol (1, 48 mg) as the main product; in a similar way, AP-1D contains the same compounds but also sugars.

The groups AP-1B and AP-1C were subjected to column chromatography using silica gel (70–230 mesh).

The AP-1B fraction (5.23 g) was adsorbed on 4.9 g of silica gel and placed in a glass column (70 cm high and 3.5 cm in diameter) packed with 157 g of silica gel. Elution was performed using a gradient system, *n*-hexane/EtOAc (100:00→50:50), and 164 fractions were obtained in 50 mL. The fractions were concentrated by reducing pressure using a rotatory evaporator; monitored by TLC; and grouped into 5 groups (AP-1B-1, AP-1B-2, AP-1B-3, AP-1B-4, and AP-1B-5).

The AP-1B-1 group (fractions 1–39, 0.306 g, *n*-hexane: EtOAc 95:05 to 85:15) was purified and identified as *O*-methylenecalinol (**1**, 32 mg) as the main product. From AP-1B-2 (fractions 40–69, 3.32 g, *n*-hexane: EtOAc 80:20 to 70:30), 7-hydroxiencalin (**3**, 7 mg) and 8-hydroxiencalin (**4**, 6 mg) were identified. The compounds encalin (**2**, 16 mg), 3,5-diprenyl-4-hydroxyacetophenone (**5**, 32 mg), and (+)- β -eudesmol (**6**, 8 mg) were isolated from the AP-1B-3 group (fractions 70–99, 0.391 g, *n*-hexane: EtOAc 65:35 to 55:45). The AP-1B-4 group (fractions 100–129, 0.821 g, *n*-hexane: EtOAc 50:50 to 40:60) led to the identification of the compounds (+)- β -eudesmol (**6**, 7 mg), dehydrospeletone (**8**, 12 mg), and speletone (**7**, 14 mg). Through successive chromatography of the AP-1B-5 group (fractions 130–149, 0.427 g, *n*-hexane: EtOAc 35:75 to 25:75), encalinol (**9**, 28 mg) and 5-acetyl-3 β -angeloxy-2 β -(1-hydroxyisopropyl)-2,3-dihydrobenzofuran (**10**, 36 mg) were isolated.

O-Methylenecalinol (**1**)

Colorless oil; ¹H-NMR (200 MHz, CDCl₃), δ_{H} : 6.95 (1H, s, H-5), 6.32 (1H, s, H-8), 6.26 (1H, d, *J* = 9.6 Hz, H-4), 5.43 (1H, d, *J* = 10 Hz, H-3), 4.61 (1H, q, *J* = 12.8, 6.8 Hz, H-11), 3.75 (3H, s, -OMe), 3.21 (3H, OMe), 1.40 (3H, s, CH₃-13), 1.39 (3H, s, CH₃-14), 1.34 (3H, d, *J* = 6.8 Hz, CH₃-12). ¹³C-NMR (50 MHz, CDCl₃). δ_{C} : 157.70 (C-7), 153.25 (C-10), 127.76 (C-3), 124.06 (C-5), 122.30 (C-4), 120.02 (C-6), 114.19 (C-9), 99.43 (C-8), 76.55 (C-2), 72.97 (C-11), 56.59 (-OMe-C11), 56.03 (OMe-C-7), 28.32 (C-13), 28.26 (C-14), 22.65 (C-12); these data match those in the literature [10,35]. The spectra of ¹H and ¹³C-NMR are shown in Figures S1 and S2.

Encalin (**2**)

Yellow oil; ¹H-NMR (400 MHz, CDCl₃), δ_{H} : 7.23 (1H, s, H-5), 6.27 (1H, s, H-8), 6.12 (1H, d, *J* = 9.8 Hz, H-4), 5.44 (1H, d, *J* = 9.7 Hz, H-3), 3.55 (3H, s, -OMe), 2.10 (3H, s, CH₃-12), 1.20 (6H, s, CH₃-13 and CH₃-14). ¹³C-NMR (100 MHz, CDCl₃). δ_{C} : 197.68 (C-11), 161.37 (C-7),

158.28 (C-10), 128.94 (C-5), 128.36 (C-3), 121.36 (C-4), 120.42 (C-6), 114.22 (C-9), 99.76 (C-8), 77.21 (C-2), 55.72 (MeO-), 32.26 (C-12), 26.68 (C-13), 28.32 (C-14); these data match those in the literature [36,37]. The spectra of ^1H and ^{13}C -NMR are shown in Figures S3 and S4.

Euparoriochromene (3)

Yellow needles; mp: 78–80 °C; ^1H -NMR (200 MHz, CDCl_3), δ_{H} : 7.21 (1H, s, H-5), 6.24 (1H, s, H-8), 6.21 (1H, d, $J = 10$ Hz, H-4), 5.41 (1H, d, $J = 10$ Hz, H-3), 2.49 (3H, s, CH_3 -12), 1.39 (6H, s, CH_3 -13 and CH_3 -14). ^{13}C -NMR (50 MHz, CDCl_3). δ_{C} : 198.13 (C-11), 162.18 (C-7), 159.18 (C-10), 128.68 (C-5), 128.53 (C-3), 126.14 (C-6), 122.08 (C-4), 114.38 (C-9), 104.26 (C-8), 77.43 (C-2), 32.12 (C-12), 28.86 (C-13), and 28.78 (C-14); these data match those in the literature [38]. The spectra of ^1H and ^{13}C -NMR are shown in Figures S2 and S5.

6-Acetyl-8-Hydroxy-2,2-Dimethylchromene (4)

White powder; mp: 98 °C; ^1H -NMR (200 MHz, CDCl_3), δ_{H} : 7.62 (1H, d, $J = 1.2$ Hz, H-7), 7.43 (1H, d, $J = 1.2$ Hz, H-5), 6.34 (1H, d, $J = 10.2$ Hz, H-4), 5.71 (1H, d, $J = 10$ Hz, H-3), 2.56 (3H, s, CH_3 -12) and 1.43 (6H, s, CH_3 -13 and CH_3 -14). ^{13}C -NMR (50 MHz, CDCl_3). δ_{C} : 202.98 (C-11), 165.23 (C-8), 160.68 (C-10), 128.61 (C-6), 128.32 (C-3), 125.34 (C-9), 122.24 (C-4), 118.38 (C-5), 114.31 (C-7), 78.26 (C-2), 28.58 (C-13 and C-14), and 26.38 (C-12); these data match those in the literature [39,40]. The spectra of ^1H and ^{13}C -NMR are shown in Figures S7 and S8.

3,5-Diprenyl-4-Hydroxyacetophenone (5)

Crystalline solid; mp: 93–95 °C; ^1H -NMR (400 MHz, CDCl_3), δ_{H} : 7.44 (2H, s, H-2 y H-6), 5.98 (1H, s, OH), 5.31 (2H, m, H-2' y H-2''), 3.37 (2H, d, $J = 7.1$ Hz, H-1' y H-1''), 2.48 (3H, d, $J = 19.8$ Hz, CH_3 -8), 1.74 (12H, d, $J = 11.1$ Hz, CH_3 -4', CH_3 -4'' y CH_3 -5', CH_3 -5''). ^{13}C -NMR (100 MHz, CDCl_3), δ_{C} : 197.52 (C-7), 157.59 (C-4), 135.28 (C-1), 130.15 (C-31, C-3''), 129.02 (C-2, C-6), 127.30 (C-3, C-5), 121.58 (C-2', C-2''), 29.82 (C-1', C-1''), 26.51 (C-8), 25.99 (C-5'', C-4'), and 18.10 (C-4'', C-5'); these data match those in the literature [41,42]. The spectra of ^1H and ^{13}C -NMR are shown in Figures S9 and S10.

β -Eudesmol (6)

White amorphous solid; mp = 78–79 °C; ^1H -NMR (200 MHz, CDCl_3), δ_{H} : 4.70 (1H, d, $J = 2$ Hz, H-15b), 4.43 (1H, d, $J = 1.6$ Hz, H-15a), 2.38 (2H, m, Hs-3), 1.98 (1H, m, H-10), 1.25–1.62 (6H, m, CH_2 -5, CH_2 -7 and CH_2 -8), 1.00–1.36 (5H, m, CH_2 -1, CH_2 -2 and CH-6), 1.39 (3H, s, CH_3 -11), 1.40 (3H, s, CH_3 -12), 0.69 (3H, s, CH_3 -14). ^{13}C -NMR (50 MHz, CDCl_3), δ_{C} : 152.41 (C-4), 105.14 (C-15), 72.23 (C-11), 49.58 (C-10), 49.42 (C-6), 42.12 (C-3), 41.86 (C-1), 41.12 (C-8), 36.89 (C-9), 26.76 (C-12 and C-13), 24.73 (C-5), 23.45 (C-2), 22.76 (C-7), and 16.24 (C-14); these data match those in the literature [43,44]. The spectra of ^1H and ^{13}C -NMR are shown in Figures S11 and S12.

Speletone (7)

Colorless oil; ^1H -NMR (200 MHz, CDCl_3), δ_{H} : 8.09 (1H, d, $J = 2.4$ Hz, H-2), 7.78 (1H, dd, $J = 2.2, 7.8$ Hz, H6), 6.84 (1H, d, $J = 8.4$ Hz, H-5), 3.60 (3H, s, OMe), 2.67 (2H, d, $J = 7.8$ Hz, H-10), 2.33 (3H, s, CH_3 -8), 2.21 (1H, m, H-11), 0.78 (6H, d, $J = 6.8$ Hz, CH_3 -12, and CH_3 -13); these data match those in the literature [40]. The spectra of ^1H -NMR are shown in Figure S13.

Dehydrospeletone (8)

Colorless oil; ^1H -NMR (200 MHz, CDCl_3), δ_{H} : 8.16 (1H, d, $J = 2.2$ Hz, H-2), 8.06 (1H, dd, $J = 2.2, 7.8$ Hz, H6), 6.98 (1H, d, $J = 8.2$ Hz, H-5), 6.56 (1H, q, H-10), 3.92 (3H, s, OMe), 2.55 (3H, s, CH_3 -8), 2.22 (3H, s, CH_3 -12), and 1.95 (3H, s, CH_3 -13); these data match those in the literature [41,42]. The spectra of ^1H -NMR are shown in Figure S14.

Encecalinalol (9)

Yellow oil; $[a]_D^{25}$: -77° (c 0.92, CHCl₃); ¹H-NMR (400 MHz, CDCl₃), δ_H : 6.95 (s, H-5), 6.37 (s, H-8), 6.27 (d, $J = 9.7$ Hz, H-4), 5.47 (d, $J = 9.8$ Hz, H-3), 5.02 (q, $J = 6.5$ Hz, H-13), 3.81 (s, MeO-), 1.47 (d, $J = 6.5$ Hz, CH₃-12), 1.42 (6H, s, CH₃-13 and CH₃-14). ¹³C-NMR (100 MHz, CDCl₃) δ_C : 157.26 (C-7), 153.18 (C-10), 127.64 (C-3), 125.76 (C-6), 123.83 (C-5), 122.02 (C-4), 113.75 (C-9), 99.53 (C-8), 77.06 (C-2), 65.53 (C-11), 55.45 (MeO-7), 28.04 (C-13), 27.96 (C-14), 22.86 (CH₃-12); these data match those in the literature [6,35,45]. The spectra of ¹H and ¹³C-NMR are shown in Figures S15 and S16.

5-Acetyl-3 β --Angeloyloxy-2 β -(1-Hydroxyisopropyl)-2,3-Dihydrobenzofurane (10)

Yellow oil; $[a]_D^{25}$ = +47 (c = 0.8, CHCl₃); ¹H NMR (400 MHz, CDCl₃), δ_H : 7.86 (d, $J = 2.1$ Hz, H-4), 7.82 (dd, $J = 8.6, 2.2$ Hz, H-6), 6.88 (d, $J = 8.6$ Hz, H-7), 6.24 (m, H-3'), 5.96 (d, $J = 7.5$ Hz, H-3), 3.88 (d, $J = 7.5$ Hz, H-2), 2.52 (s, CH₃-14), 2.04 (dq, $J = 7.3, 1.5$ Hz, CH₃-4'), 1.93 (p, $J = 1.5$ Hz, CH₃-5'), 1.51 (s, CH₃-11), 1.35 (s, CH₃-12). ¹³C-NMR (100 MHz, CDCl₃), δ_C : 196.49 (C-13), 169.43 (C-1'), 157.12 (C-9), 141.17 (C-3'), 132.48 (C-5), 130.42 (C-4), 129.76 (C-6), 126.81 (C-2'), 119.53 (C-8), 117.49 (C-7), 79.60 (C-10), 74.03 (C-2), 71.73 (C-3), 26.29 (C-12), 25.88 (C-14), 20.58 (C-5'), 19.73 (C-13), and 16.12 (C-4'); these data match those in the literature [6,10]. The spectra of ¹H and ¹³C-NMR are shown in Figures S17 and S18.

2.2.2. Purification and Identification of Compounds from *A. pichinchensis* Flowers

Selected flowers from the collected plants were dried in the shade at room temperature. The plant material (256.7 g) was successively extracted with ethanol/H₂O (95:05 *v/v*) three times (each time with 4 L of the solvent). The hydroalcoholic extract obtained was concentrated to dryness by distillation under reduced pressure using a rotary evaporator, obtaining 6.7 g of residue.

Fractionation of the hydroalcoholic extract by open CC (silica gel, 70–230 mesh; 10 cm i.d. \times 60 cm) was performed with a gradient system of *n*-hexane-CH₂Cl₂/MeOH 90:10:00 to 100% MeOH. Fractions of 100 mL were obtained (53 fractions). Based on TLC analysis, these fractions were grouped according to their chemical profile into two main groups: AP-M-1A (1–32, 2.02 g) and AP-M-1B (33–53, 3.98 g). The groups were subjected to column chromatography using silica gel (70–230 mesh).

The AP-M-1A fraction was adsorbed on 3 g of silica gel and placed in a glass column (80 cm high and 3.5 cm in diameter) packed with 70 g of silica gel. Elution was carried out using a gradient system, *n*-hexane/CH₂Cl₂ (100:00 \rightarrow 80:20), and 37 fractions, each comprising 100 mL, were obtained. These were concentrated and monitored by TLC and grouped into three groups of fractions: AP-M-1A-1 (fractions 1–17, 0.87 g), AP-M-1A-2 (fractions 18–26, 0.606 g), and AP-M-1A-3 (fractions 27–37, 0.87 g).

The three groups of fractions were subjected to successive purification processes using a gradient system (CH₂Cl₂/MeOH 95:05 to 80:20), obtaining *O*-methylencecalinalol (**1**, 32.4 mg) as the main product from the AP-M-1A-1 fraction; encocalin (**2**, 24 mg) and 3, 5-diprenyl-4-hydroxyacetophenone (**5**, 16 mg) were from the AP-M-1A-2 group; and spetone (**7**, 14 mg), dehydrospletone (**8**, 11 mg), encecalinalol (**9**, 17 mg), and betuletol 3-*O*- β -glucoside (**11**, 64 mg) were purified from the AP-M-1A-3 group.

Betuletol 3-*O*- β -Glucoside (11)

Yellow amorphous solid; mp: 152–154 °C; ¹H-NMR (500 MHz, DMSO-*d*₆); δ_H : 12.58 (1H, s, OH), 8.00 (2H, d, $J = 8.9$ Hz, H-2' H-6'), 6.90 (1H, s, H-8), 6.82 (2H, d, $J = 8.9$ Hz, H-3' H-5'), 5.25 (1H, d, $J = 7.7$ Hz, H-1''), 3.85 (3H, s, OMe-H-4'), 3.70 (3H, s, OMe-H-6), 3.58–3.56 (1H, ddd, $J = 9.7, 7.7, 4.7$ Hz, H-4''), 3.32–3.31 (1H, m, H-5''), 3.37–3.36 (1H, m, H-3''), 3.47–3.45 (1H, m, H-2''), 3.33–3.29 (1H, m, H-6''). ¹³C-NMR (125 MHz, DMSO-*d*₆), δ_C : 177.86, (C-4), 160.13, (C-4'), 158.80 (C-7), 156.78, (C-2), 151.81 (C-5), 151.68 (C-9), 133.29 (C-3), 131.76 (C-6), 128.57 (C-2', C-6'), 120.65 (C-1'), 115.56 (C-3', C-5'), 105.36 (C-10), 101.99 (C-1''), 91.82 (C-8), 73.95 (C-5''), 73.54 (C-3''), 74.13 (C-2''), 70.59 (C-4''), 60.63 (C-6''), 60.64 (C-OMe-6), 56.97 (C-OMe-4'); these data match those in the literature [46,47]. The spectra

of ^1H and ^{13}C , DEPT, and HMBC NMR are shown in Figures S19–S22. $\text{C}_{23}\text{H}_{25}\text{O}_{12}$ (MSFAB⁺ $m/z = 493$) MS is shown in Figure S23.

2.3. Anti-Inflammatory Assays

2.3.1. TPA-Induced Mouse Ear Edema

Male CD1 mice (6 to 8 weeks of age) were used. The sample size was five animals for each test group, according to the method described previously. The mice were maintained under standard laboratory conditions (Biotherium of the School of Medicine, Universidad Autónoma del Estado de Morelos) at $22\text{ }^\circ\text{C} \pm 3\text{ }^\circ\text{C}$, $70\% \pm 5\%$ humidity, 12 h light/dark cycle, and food/water ad libitum. The experimental protocol used was approved by Comité para el Cuidado y Uso de los Animales del Laboratorio (CCUAL) de la Facultad de Medicina (No. 06-2015). For control, the left ear (Wt) was treated with 2.5 g/ear of 12-O-Tetradecanoylphorbol 13-acetate (TPA, St. Louis, MO, USA), dissolved in 20 μL of acetone applied to the inner and outer surface, and the right ear (Wnt) was treated with the vehicle acetone. Sample doses of 0.1 mg/ear of the extracts, as well as the reference anti-inflammatory drug indomethacin, were applied. All samples were dissolved in 10 μL acetone and applied topically to the right ear immediately after TPA application; acetone was applied as a vehicle to the left ear. Four hours after the application of the samples, the animals were sacrificed by cervical dislocation. Biopsies were taken with a 6 mm diameter punch from both treated (t) and untreated (nt) ears to determine inflammation. The following formula determined the percent of inhibition:

$$\text{Inhibition\%} = \left(\frac{\Delta w_{\text{control}} - \Delta w_{\text{treatment}}}{\Delta w} \right) \times 100$$

where $\Delta w = w_t - w_{nt}$; w_t is the weight (grams) of the section of the treated ear, and w_{nt} is the weight of the section of the non-treated ear [34,48].

2.3.2. In Vitro Anti-Inflammatory Activities

The in vitro anti-inflammatory activity was evaluated using the in vitro model of nitric oxide inhibition of the RAW 264.7 macrophage cell line. For this purpose, the cell line was cultured in 75 cm^2 flasks; subsequently, the cell viability was determined by MTS, applying the treatments (pure compounds at different concentrations) to determine whether the compounds inhibit cell viability. Next, macrophages were cultured in 96-well plates, and their nitric oxide inhibition was determined using the supernatant, with which the Griess reaction was performed, measuring nitrite production as an indicator of NO production in the medium, since NO is unstable under aerobic conditions. The cytokine IL-6 was determined using the PEPROTECHTM kit, while NF- κB activation was evaluated in macrophages of the RAW-BlueTM cell line.

Macrophage Culture in 75 cm^2 Flasks

The ATCC[®] Tib-71TM macrophage cell line (Georgetown, Washington, DC, USA) was cultured in the ADVANCED DMEM/F12 medium (GIBCO) + 1% GLUTAMAXTM, supplemented with 3.5% fetal bovine serum (FBS) without antibiotics, in 75 cm^2 cell culture flasks, then incubated in 5% CO_2 atmosphere at $37\text{ }^\circ\text{C}$ until 70%–90% confluence was reached. After that, the cells were detached, and 10 mL of the culture medium was applied and centrifuged at $9500 \times g$ for 5 min. The cell pellet was resuspended in 5 mL of culture medium, and cells were counted using a Neubauer camera for subculturing in 96-well culture plates.

Cell Viability of RAW 264.7 Macrophages

Macrophages were seeded in a 96-well plate (10,000 cells/well) with 0.1 mL of ADVANCED DMEM/F12 + 1% GLUTAMAXTM culture medium with 3.5% fetal bovine serum and incubated for 24 h at $37\text{ }^\circ\text{C}$ in a 5% CO_2 atmosphere. After the incubation time, the compounds (1–11) were dissolved in dimethyl sulfoxide (DMSO) and filtered through

0.45 µm cellulose membranes, and the compounds were added at different concentrations. The vehicle DMSO at 0.5% *v/v* and etoposide at 40 and 20 µg/mL were incubated for 20 h [32,33]. Then, 20 µL of MTS [3-(4,5-dimethylthiazol-2-yl)-5-(3-carboxymethoxyphenyl)-2-(4-sulfophenyl)-2H-tetrazolium] reagent (CellTiter 96 Aqueous Non-Radioactive Cell Proliferation Assay PROMEGA) was added to each of the wells and incubated for 4 h. Finally, the optical density was measured at 490 nm in an ELISA plate reader (Epoch microplate spectrophotometer, Bio-Tek, Santa Clara, CA, USA) [49,50].

Treatment of Macrophages with Compounds and LPS

Macrophages (30,000 cells/well) were seeded in a 96-well cell culture plate with 0.2 mL of ADVANCED DMEM/F12+ 1% GLUTAMAX™ culture medium with 3.5 fetal bovine serum and incubated for 24 h in a 5% CO₂ atmosphere at 37 °C. Subsequently, the compounds were applied at 150, 75, 37.5, 18.8, and 9.4 µM; indomethacin (positive control) at 85 µM; and the vehicle DMSO at 0.5% and incubated for 2 h. Next, 2 µg/mL of lipopolysaccharide (LPS) was added and incubated for 24 h. Finally, the supernatant was removed by placing 50 µL of each well in an ELISA plate for the Griess reaction, and 100 µL of supernatant was reserved for the cytokine analysis.

Determination of NO in RAW 264.7 Macrophages

Next, 50 µL of each previously obtained supernatant was used and mixed with 100 µL of Griess reagent (50 µL of 1% sulfanilamide and 50 µL of N-(1-naphthyl) ethylenediamine dichlorohydrate 0.1% in 2.5% phosphoric acid) for 10 min. Finally, the optical density was measured at 540 nm with a plate reader, and the concentration of nitrite present in the samples was calculated by comparing it with the optical density of a NaNO₂ standard curve prepared in a fresh medium [33,34,44].

Determination of the IL-6 Concentration in RAW 264.7 Macrophages

The anti-inflammatory effect of compound **11** was analyzed in RAW 264.7 cells treated with LPS. Cells were seeded in 96-well plates at a density of 3×10^4 cells/well incubated for 24 h. The cells were expressed with 1 µg/mL of LPS and compound **11** at concentrations of 37.5, 75, and 150 µg/mL for 24 h. The IL-6 levels in the cell culture medium were measured using an Elisa kit following the manufacturer's instructions (Biosciences Pharmingen, San Diego, CA, USA) [49–51].

RAW-Blue Cell Culture

RAW-Blue cell line macrophages (RAW-Blue InvivoGen) were cultured in the DMEM/F12 medium (GIBCO) supplemented with 10% fetal bovine serum (GIBCO) with 1% MycoZap (Lonza) and 200 µg/mL zeotín, which were incubated in 75 cm² cell culture flasks in a 5% CO₂ humidified atmosphere at 37 °C until 70%–80% cell confluence was reached. Cells were then detached by removing the supernatant, and 1.5 mL of trypsin (GIBCO) was applied. The cells were then centrifuged, the cell pellet was resuspended with 5 mL of the medium, and cell counting was performed using a Neubauer camera.

RAW-Blue Macrophage Treatment

RAW-Blue cells were seeded in 96-well plates (30,000 cells per well) with 0.1 mL of DMEM/F12 medium containing 10% fetal bovine serum with 1% antibiotic (MycoZap) and 200 µg/mL zeotín and incubated for 24 at 37 °C in a 5% CO₂ atmosphere. Macrophages were then incubated with the test compounds for 2 h at the maximum noncytotoxic concentration that showed an inhibitory effect on NO production. After being incubated with LPS at 10 µg/mL (for wells with compounds and 100% control), a proinflammatory stimulus and without LPS (negative control) at 37 °C for 20 h was used to stimulate NF-κβ activation. Finally, cell-free supernatants were collected and used fresh to determine NF-κβ activation by a reaction with QUANTI-Blue™. This assay allows for the detection of NF-κβ/AP-1 in the RAW-Blue system. Alkaline phosphatase activity (AP) was used as an indicator of NF-

$\kappa\beta$ activation in the supernatants (culture medium) by using QUANTI-Blue (InvivoGen), according to the instructions provided by the manufacturer [49,50].

2.4. Statistical Analysis

The results shown were obtained through at least three independent experiments and were presented as means \pm SDs. Statistical analyses were performed using one-way analysis of variance (ANOVA) followed by Dunnett's multiple comparisons test. All statistical analyses were performed using GraphPad Prism, version 6.0 software. p -values < 0.05 were considered to indicate statistical significance [34].

3. Results and Discussion

3.1. Anti-Inflammatory Activity of the Extract from the Aerial Parts of *A. pichinchensis*

Topical application of the extracts (0.1 mg/ear) to the mice resulted in the potent suppression of acute edema induced by TPA. Ethyl acetate and methanol extracts from leaves and stems, as well as a hydroalcoholic extract (95:05 v/v) from the flowers of *Ageratina pichinchensis*, were evaluated in an in vivo model of inflammation (Figure 1). The best inhibitory effect was presented by the ethyl acetate leaf extract (85.27% \pm 4.44) and hydroalcoholic flower extract (83.62% \pm 5.00), being statistically comparable with the positive control indomethacin (91.19% \pm 2.60).

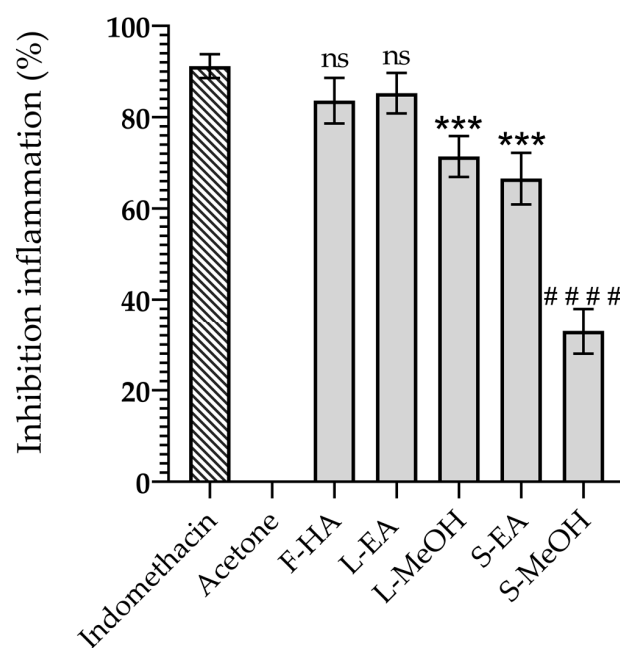


Figure 1. Anti-inflammatory effect of in vivo extracts of leaves and stems of *A. pichinchensis*. F-HA: ethanol:H₂O (95:05 v/v): hydroalcoholic ethanolic extract of flowers; L-EA: ethyl acetate extract of leaves; L-MeOH: methyl extract of leaves; S-EA: ethyl acetate extract of stems; S-MeOH: methyl extract of stems. Data are expressed as mean \pm SD values of experiments in three independent assays. Significance was determined using ANOVA followed by Dunnett's multiple comparisons test. *** $p < 0.001$, ns: not significant vs. indomethacin-treated extracts, and #### $p < 0.001$ vs. vehicle acetone.

These results led to the fractionation and isolation of the secondary metabolites present in the leaves (EtOAc) and flower extracts for further biological evaluation to identify the compounds responsible for the effect shown by the active extracts.

3.2. Chemical Composition of Anti-Inflammatory Extracts

The ethyl acetate (leaves) and hydroalcoholic (flowers) extracts obtained from *A. pichinchensis* were subjected to successive purification processes using the column chro-

matography technique and normal phase silica gel, which led to the isolation of pure compounds that were identified by analysis of their spectroscopic data and comparison with data from the literature. All the identified compounds are known and have been reported in different species of the *Ageratina* genus. At the extract level, different biological effects have been demonstrated.

From the ethyl acetate extract (leaves), the following were identified: *O*-methylenecalinalol (1) [10,35], enecalinalol (2) [36,37], eupatoriocromene (3) [38], 6-acetyl-8-hydroxy-2,2-dimethylchromene (4) [33,40], 3,5-diprenyl-4-hydroxyacetophenone (5) [41,42], (+)- β -eudesmol (6) [43,44], espeletone (7) [40], dehydrospeletone (8) [41,42], enecalinalol (9) [6,35,45], and 5-acetyl-3 β -angeloyloxy-2 β -(1-hydroxyisopropyl)-2,3-dihydrobenzofuran (10) [6,10]. In the hydroalcoholic extract (flowers), in addition to some compounds (1, 2, 5, and 6), betuletol 3-*O*- β -glucoside (11) was identified [46,47].

Compounds (3, 4, and 11) were isolated from this plant for the first time, and we investigated the abilities of compounds 1–11 (Figure 2) to inhibit NO production.

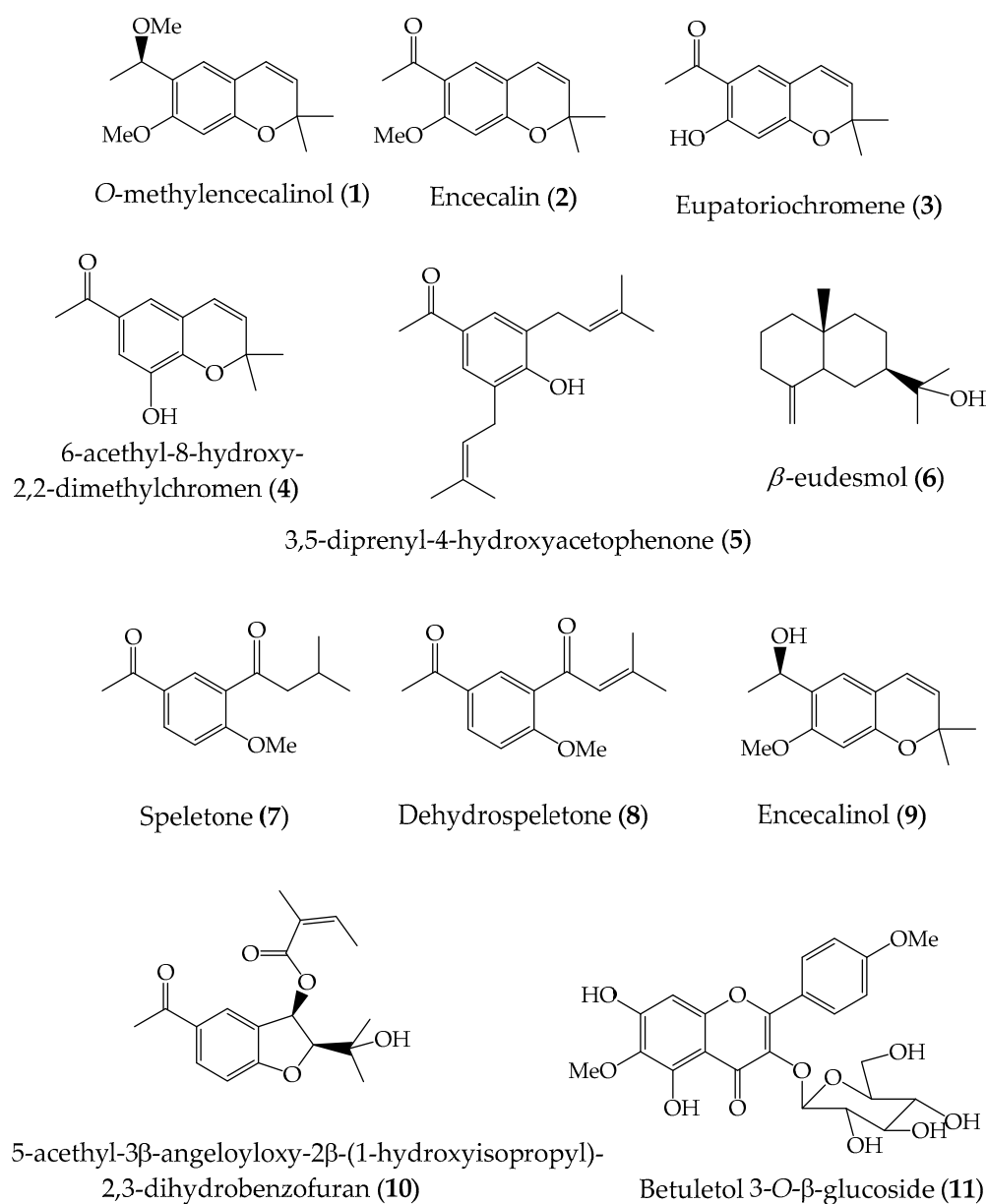


Figure 2. Compounds isolated from aerial parts of *A. pichinchensis*.

Compound **3** has been reported in the species *Centaurea solstitialis* L., *Caccinia macranthera* Brand var. *macranthera*, *Calea serrata*, *Encelia farinose*, *Helianthus annuus*, and *Piper mollicomum* Kunth [36,52–56]. Regarding compound **4**, it has been reported in the species *Titinia diversifolia* and *Ageratum houstonianum* [38,57], while compound **11** has been reported in the species *Arnica montana* [46,47].

The compounds identified in our study have been widely described chemically by different authors; however, there is little information on the chemical characterization of compound **11**, and, therefore, we will provide more information on its structural elucidation in this study.

Compound **11** was obtained as a yellow-colored amorphous solid. The elucidation of its chemical structure involved a comprehensive analysis using ^1H , ^{13}C , and DEPT NMR (Figures S1–S3), along with a two-dimensional heteronuclear HMBC experiment (Figure S4) as well as a FAB+ mode mass spectrometry analysis (Figure S5). In the ^1H NMR spectrum, an AA'BB' aromatic spin system was evidenced by the two doublets, as there were two doublet signals at δ 6.88 and δ 8.12 with coupling constants of $J = 8.7$ Hz and 8.9 Hz, respectively. Additionally, a singlet signal at δ 6.9 was assigned to a penta-substituted benzene. Another doublet signal at δ 5.44 was also observed in the spectrum ($J = 7.7$ Hz), as well as several signals between δ 3.5 and δ 4.5, characteristic of a glucopyranose; these signals were evident in the ^{13}C NMR spectrum, indicating that the aglycone was glycosylated. Once these signals were assigned, it was established that it was a glycosylated flavonol and that, based on the HMBC experiment (Figure S5), the sugar molecule was connected to the oxygen in the 3-position of the aglycone. Once the structural identity was established, the yellow solid was identified as betuletol 3-O- β -glucoside.

After identifying the compounds present in the aerial parts of *A. pichinchensis*, the anti-inflammatory effect was evaluated with the in vitro model of nitric oxide inhibition to identify the chemical principles associated with this effect attributed to traditional medicine.

3.3. Inhibition of LPS-Induced NO Production by Compounds 1–11

The compounds were solubilized in DMSO and evaluated at concentrations of 9.375, 18.75, 37.50, 75.00, and 150.00 μM (Table S1). Table 1 shows the effect found for the compounds at a concentration of 75 μM , highlighting that only compound **6** exhibited a cytotoxic effect at this concentration. The rest of the compounds did not reveal an important reduction in cell viability compared to the positive control (etoposide) at the concentrations evaluated (Table S2).

Table 1. Percentage of inhibition of NO production and cell viability in RAW 264.7 macrophages at a concentration of 75 μM for compounds 1–11.

Compounds	Cell Viability (%) ^a	NO Inhibition 75 μM (%)	NO Inhibition (IC ₅₀ , μM)
1	109.9 \pm 7.16	0.95 \pm 1.35	>75
2	112.4 \pm 24.08	16.75 \pm 5.36	>75
3	115.6 \pm 1.58	11.98 \pm 7.85	>75
4	99.33 \pm 12.39	22.63 \pm 10.38	>75
5	100.20 \pm 2.95	29.77 \pm 18.27	>75
6	61.14 \pm 6.31	----	----
7	104.7 \pm 1.82	5.90 \pm 8.35	>75
8	103.9 \pm 3.83	36.73 \pm 16.93	>75
9	110.9 \pm 8.3	29.77 \pm 9.37	>75
10	121.2 \pm 10.20	5.98 \pm 5.22	>75
11	101.3 \pm 1.62	75.08 \pm 3.07	20.55 \pm 0.27
DMSO ^b	----	----	----
Indomethacin ^c (84 μM)	----	65.93 \pm 6.03	54.69 \pm 10.34
Etoposide ^d (68 μM)	42.02 \pm 4.23	----	----

^a Cell viability at 75 μM ; ^b blank control; ^c positive control for the NO production assay; ^d positive control for cytotoxicity against RAW 264.7 cells.

Compound **6** was not evaluated to determine its effect on NO production, because it only promoted a survival rate of 61.14% at a concentration of 75 μM . β -eudesmol is a sesquiterpene that has already been isolated from several species; to mention a few, there are *Atractylodes lancea* [58], *Zingiber Zerumbet* [59], *Gutteria friesiana* [60], and *Murraya tetramera* [61]. Likewise, several biological effects have been demonstrated for this secondary metabolite, for which we can highlight its anti-inflammatory effect, tumor suppressor effect, and anticancer effect [62–64]. The above agrees with the inhibitory effect that compound **6** had on cell viability.

Therefore, we proceeded to evaluate the inhibitory effect of compounds **1–5** and **7–11** on the production of NO in RAW 264.7 macrophages previously stimulated with LPS for 24 h after 2 h of incubation.

The results revealed that the NO level was increased in RAW 264.7 cells with LPS stimulation, and this effect was significantly decreased by treatment with the compounds. The inhibition percentages and IC_{50} values are shown in Table 1. It was observed that compound **11** was the best inhibitor of NO secretion, with an IC_{50} of 20.55 ± 0.27 , and it competed with indomethacin, which IC_{50} value was 54.69 ± 10.34 .

Regarding specifically the activity displayed by compound **11**, it was observed that it presents a dose-dependent effect (Figure 3a), even improving the inhibition exhibited by the positive control indomethacin. Consequently, its relationship with the proinflammatory cytokine IL-6 and the nuclear factor NF- κB was determined. The results indicate a statistically significant inhibition of interleukin IL-6; likewise, NF- κB activation is also inhibited (Figure 3b,c). This result suggests that compound **11** exhibits a proinflammatory effect which application could represent alternatives for the treatment of diseases such as rheumatoid arthritis, chronic hepatitis, pulmonary fibrosis, sepsis, and hypertension, among others [65–68].

Compound **11**, like some essential oils, showed an anti-inflammatory effect, demonstrated by the inhibition of nitric oxide associated with regulating the expression of proinflammatory cytokines [69,70]. Other compounds have shown similar effects to compound **11** in the same inflammation model, such as the case of the compound 4-methoxycinnamyl *p*-coumarate isolated from the species *Etilingera pavieana*, which revealed an IC_{50} of $15.0 \pm 1.4 \mu\text{M}$ [71]. On the other hand, the triterpene methyl lucidenate L isolated from the species *Ganoderma lucidum* exhibited an IC_{50} of $36.8 \pm 1.0 \mu\text{M}$ [72]. It should be noted that compound **11** has not been reported in *Ageratina* species, although it has been reported in species of the Asteraceae family, for example, in the species *Arnica montana* and *Arnica chamissonis*, and both plants have been used in traditional medicine as healing and anti-inflammatory agents at the extract level [46,47]. These species are characterized by containing sesquiterpene lactones, such as helenalin, $11\alpha,13$ -dihydrohelenalin, and chamissonolide, which inhibit the activation of transcription factor NF- κB [73].

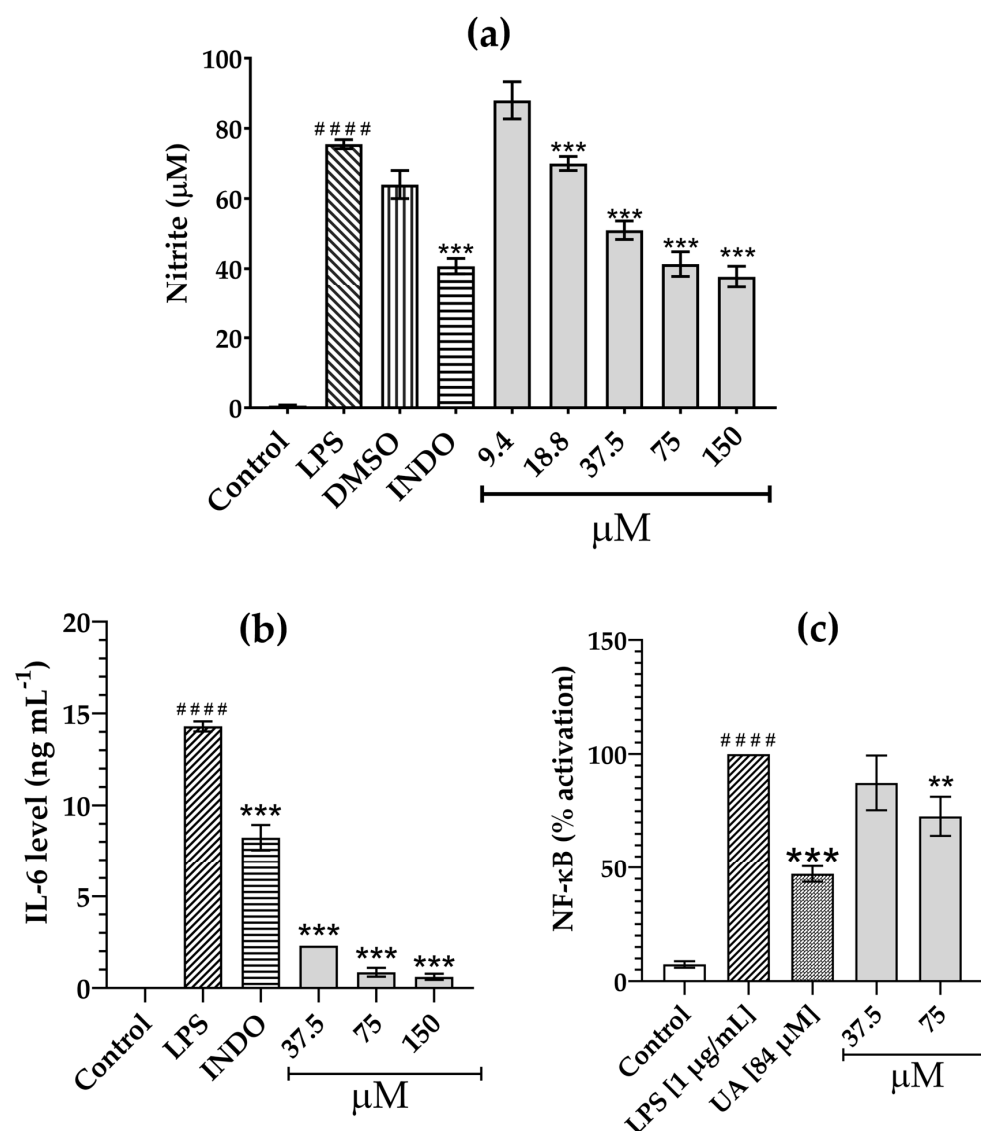


Figure 3. Effect of compound **11** on (a) NO, (b) IL-6, and (c) NF-κβ of RAW 264.7 macrophages activated with LPS. Data were expressed as the mean ± SD values of experiments in three independent assays. ** $p < 0.01$, *** $p < 0.001$ vs. LPS-treated cells, and #### $p < 0.001$ vs. vehicle control.

4. Conclusions

For the first time, we report the anti-inflammatory effect of *A. pichinchensis*, specifically the ethyl acetate extracts of leaves and ethanolic extracts of flowers, which exhibited in vivo anti-inflammatory effects, significantly inhibiting TPA-induced edema at a dose of 0.01 per ear. Additionally, the inhibitory effect on NO production in an in vitro inflammatory model of compounds **1–5** and **7–11**, isolated from the leaves and flowers of *A. pichinchensis*, was evaluated. Among them, betuletol 3-O-β-glucoside (**11**) inhibited NO production in a dose-dependent manner; in particular, treatment with 75 μM significantly decreased NO production by $75.08 \pm 3.07\%$ ($IC_{50} = 20.55 \pm 0.27$) compared to indomethacin, which inhibition was $65.93 \pm 6.03\%$ ($IC_{50} = 54.69 \pm 10.34$). The nitric oxide inhibition effect associated with the upregulation of proinflammatory cytokine (IL-6) expression and inhibition of NF-κβ activation indicates that compound **11** may be useful as a therapeutic agent in the treatment of inflammation-related diseases caused by macrophage overactivation. Therefore, the effect attributed to *A. pichinchensis* species is due to compound **11**, and these findings corroborate the effect attributed to the species in traditional medicine.

Supplementary Materials: The following supporting information can be downloaded at <https://www.mdpi.com/article/10.3390/app14093942/s1>: Tables S1 and S2. Effect of compounds 1–11 at different concentrations on cell viability and NO production in RAW 264.7 cells. Figures S1–S12 and S15–S18. ¹H and ¹³C NMR spectra of compounds 1–6 and 9 and 10. Figures S13 and S14. ¹H NMR spectra of compounds 7 and 8. Figures S19–S22. One-dimensional and two-dimensional NMR spectra of compound 11. Figure S23. Mass–mass spectrum (FAB+).

Author Contributions: Conceptualization, S.M.-B. and F.C.-S.; formal analysis, A.R.-E., A.R.-G. and J.G.-C.; funding acquisition, F.C.-S., J.J.A.-F. and L.A.; investigation, M.S.-R. and S.M.-B.; methodology, J.J.A.-F., A.R.-E., A.G.-A., J.G.-C. and M.S.-R.; resources, F.C.-S. and L.A.; supervision, L.A., A.R.-G., F.C.-S. and M.S.-R.; writing, S.M.-B., J.J.A.-F. and M.S.-R.; original draft, A.R.-G., L.A. and J.J.A.-F.; writing—review and editing, S.M.-B., M.S.-R., A.G.-A. and F.C.-S. All authors have read and agreed to the published version of the manuscript.

Funding: This research was supported in part by Conahcyt (Grant CB 240801).

Institutional Review Board Statement: Not applicable.

Informed Consent Statement: Not applicable.

Data Availability Statement: The data presented in this study are available on request from the corresponding author. The data are not publicly available due to privacy.

Acknowledgments: The authors thank the Laboratorio Nacional de Estructura de Macromoléculas (Conahcyt 279905) for the spectroscopic and mass analyses. The authors thank Gabriel Flores, curator of the HUMO Herbarium, for his support with the taxonomic identification.

Conflicts of Interest: The authors declare no conflicts of interest.

References

1. McVaugh, R. Compositae. Flora Novo-Galiciana. In *A Descriptive Account of the Vascular Plants of Western Mexico*; The University of Michigan Press: Ann Arbor, MI, USA, 1984; Volume 12.
2. GBFI. *Ageratina Pichinchensis*. Available online: <https://www.gbif.org/es/species/5400249> (accessed on 1 December 2023).
3. Villaseñor, R.; Espinosa, G.F.J. *Catálogo de Malezas de México*; Universidad Nacional Autónoma de México: México City, México, 1998; pp. 1–448.
4. INAH. Jardín Etnobotánico y Museo de la Medicina Tradicional. 2023. Available online: https://lugares.inah.gob.mx/es/museos-inah/colecciones/piezas/12915-12915-axihuilit.html?lugar_id=389 (accessed on 1 December 2023).
5. Argueta, A.; Cano, L.; Rodarte, M. *Atlas de la Medicina Tradicional Mexicana, Tomo 1–3*; Instituto Nacional Indigenista: Mexico City, Mexico, 1994; p. 1786.
6. Ríos, M.Y.; Aguilar-Guadarrama, B.; Navarro, V. Two new benzofurans from *Eupatorium aschenbornianum* and their antimicrobial activity. *Planta Med.* **2003**, *69*, 967–970. [[PubMed](#)]
7. Navarro-García, V.M.; Gonzalez, A.; Fuentes, M.; Aviles, M.; Ríos, M.Y.; Zepeda, G.; Rojas, M.G. Antifungal activities of nine traditional Mexican medicinal plants. *J. Ethnopharmacol.* **2003**, *87*, 85–88. [[CrossRef](#)] [[PubMed](#)]
8. Sánchez-Mendoza, M.E.; Reyes-Trejo, B.; Sánchez-Gómez, P.; Rodríguez-Silverio, J.; Castillo-Henkel, C.; Cervantes-Cuevas, H.; Arrieta, J. Bioassay-guided isolation of an anti-ulcer chromene from *Eupatorium aschenbornianum*: Role of nitric oxide, prostaglandins and sulfhydryls. *Fitoterapia* **2010**, *81*, 66–71. [[CrossRef](#)] [[PubMed](#)]
9. Sánchez-Mendoza, M.; Rodríguez-Silverio, J.; Rivero-Cruz, J.F.; Rocha-González, H.; Pineda-Farías, J.; Arrieta, J. Antinociceptive effect and gastroprotective mechanisms of 3,5-diprenyl-4-hydroxyacetophenone from *Ageratina pichinchensis*. *Fitoterapia* **2013**, *87*, 11–19. [[CrossRef](#)] [[PubMed](#)]
10. Aguilar-Guadarrama, B.; Navarro, V.; León-Rivera, I.; Ríos, M.Y. Active compounds against tinea pedis dermatophytes from *Ageratina pichinchensis* var. *bustamenta*. *Nat. Prod. Res.* **2009**, *23*, 1559–1565. [[CrossRef](#)] [[PubMed](#)]
11. Romero-Cerecero, O.; Zamilpa, A.; Jiménez, E.; Tortoriello, J. Effect on the wound healing process and in vitro cell proliferation by the medical Mexican plant *Ageratina pichinchensis*. *Planta Med.* **2011**, *77*, 979–983. [[CrossRef](#)] [[PubMed](#)]
12. Torres-Barajas, L.; Rojas-Vera, J.; Morales-Méndez, A.; Rojas-Fermín, L.; Lucena, M.; Buitrago, A. Chemical composition and evaluations of antibacterial activity of oils of *Ageratina jahnii* and *Ageratina pichinchensis* collected in Mérida, Venezuela. *Bol. Latinoam. Caribe Plant. Med. Aromat.* **2013**, *12*, 92–98.
13. Romero-Cerecero, O.; Zamilpa, A.; González-Cortazar, M.; Alonso-Cortés, D.; Jiménez-Ferrer, E.; Nicasio-Torres, P.; Aguilar-Santamaría, L.; Tortoriello, J. Pharmacological and chemical study to identify wound-healing active compounds in *Ageratina pichinchensis*. *Planta Med.* **2013**, *79*, 622–627. [[CrossRef](#)] [[PubMed](#)]
14. White, M.M.D. Mediators of inflammation and the inflammatory process. *J. Allergy Clin. Immunol.* **1999**, *103*, S978–S981. [[CrossRef](#)]
15. Duleba, M.D.A.J.; Dokras, M.D.A. Is PCOS an inflammatory process? *Fert. Steril.* **2012**, *97*, 7–12. [[CrossRef](#)]

16. Adbulkhaleq, L.A.; Assi, M.A.; Abdullah, R.; Zamri-Saad, M.; Taufiq-Yap, Y.H.; Hezme, M.N.M. The crucial roles of inflammatory mediators in inflammation: A review. *Vet. World* **2018**, *11*, 627–635. [[CrossRef](#)] [[PubMed](#)]
17. Sugimoto, M.A.; Vago, J.P.; Perretti, M.; Teixeira, M.M. Mediators of the resolutions of the inflammatory response. *Trends Immunol.* **2019**, *1545*, 1–16. [[CrossRef](#)] [[PubMed](#)]
18. Veríssimo, F.J.; Oliveira, C.R.N.; Nunes, J.C.A.; Araújo, M.F.T.A.; Veríssimo, A.J.W.; Galvao, A.J.M. The role of the mediators of inflammation in cancer development. *Pathol. Onco. Res.* **2015**, *21*, 527–534.
19. Salgado, A.; Bóveda, J.L.; Monasterio, J.; Segura, R.M.; Mourelle, M.; Gómez-Jiménez, J.; Peracaula, R. Inflammatory mediators and their influence on haemostasis. *Haemostasis* **1994**, *24*, 132–138. [[CrossRef](#)]
20. Schlag, G.; Redl, H. Mediators of injury and inflammation. *World J. Sug.* **1996**, *20*, 406–410. [[CrossRef](#)] [[PubMed](#)]
21. Bradley, T.S.; Geller, D.A. Molecular regulation of the human inducible nitric oxidase synthase (iNOS) gene. *Shock* **2000**, *13*, 413–424.
22. Krishna, R.K.M. Molecular mechanisms regulating iNOS expression in various cell types. *J. Toxicol. Environ. Health B Crit. Rev.* **2000**, *3*, 27–58.
23. Chiou, W.-F.; Chen, C.-F.; Lin, J.-J. Mechanisms of suppression of inducible nitric oxide synthase (iNOS) expression in RAW 264.7 cells by andrographolide. *Br. J. Pharmacol.* **2000**, *129*, 1553–1560. [[CrossRef](#)]
24. Aktan, F. iNOS-mediated nitric oxide production and its regulation. *Life Sci.* **2004**, *75*, 639–653. [[CrossRef](#)]
25. Poteser, M.; Wakabayashi, I. Serum albumin induces iNOS expression and NO production in RAW 264.7 macrophages. *Br. J. Pharmacol.* **2004**, *143*, 143–151. [[CrossRef](#)]
26. Anavi, S.; Tirosh, O. iNOS as a metabolic enzyme under stress conditions. *Free Radic. Biol. Med.* **2020**, *146*, 16–35. [[CrossRef](#)]
27. Xue, Q.; Yan, Y.; Zhang, R.; Xiong, H. Regulation of iNOS on immune cells and its role in diseases. *Int. J. Mol. Sci.* **2018**, *19*, 3805. [[CrossRef](#)] [[PubMed](#)]
28. Xu, W.; Liu, L.Z.; Loizidou, M.; Ahmed, M.; Charles, I.G. The role of nitric oxide in cancer. *Cell Res.* **2002**, *12*, 311–320. [[CrossRef](#)]
29. Xie, Q.-W.; Nathan, C. The high-output nitric oxide pathway: Role and regulation. *J. Leuk. Biol.* **1994**, *56*, 576–582. [[CrossRef](#)] [[PubMed](#)]
30. Nagy, G.; Clark, J.M.; Buzás, E.I.; Gorman, C.L.; Cope, A.P. Nitric oxide, chronic inflammation and autoimmune. *Immunol. Lett.* **2007**, *111*, 1–5. [[CrossRef](#)]
31. Laroux, F.S.; Pavlick, K.P.; Hines, I.N.; Kawachi, S.; Harada, H.; Bharwani, S.; Hoffman, J.M.; Grisham, M.B. Role of nitric oxide in inflammation. *Acta Physiol. Scand.* **2001**, *173*, 113–118. [[CrossRef](#)]
32. Hurtado-Díaz, I.; Sánchez-Carranza, J.N.; Romero-Estrada, A.; González-Maya, L.; González-Christen, J.; Herrera-Ruiz, M.; Alvarez, L. 16-Hydroxy-Lycopersene, a Polyisoprene Alcohol Isolated from *Tournefortia hirsutissima*, Inhibits Nitric Oxide Production in RAW 264.7 Cells and Induces Apoptosis in Hep3B Cells. *Molecules* **2019**, *24*, 2366. [[CrossRef](#)] [[PubMed](#)]
33. Romero-Estrada, A.; Maldonado-Magaña, A.; González-Christen, J.; Marquina Bahena, S.; Garduño-Ramírez, M.L.; Rodríguez-López, V.; Alvarez, L. Anti-inflammatory and antioxidative effects of six pentacyclic triterpenes isolated from the Mexican copal resin of *Bursera copallifera*. *BMC CAM* **2016**, *16*, 422. [[CrossRef](#)]
34. Sánchez-Ramos, M.; Marquina, B.S.; Romero-Estrada, A.; Bernabé-Antonio, B.; Cruz-Sosa, F.; González-Christen, J.; Acevedo-Fernández, J.J.; Perea-Arango, I.; Alvarez, L. Establishment and phytochemical analysis of a callus cultures from *Ageratina pichinchensis* (Asteraceae) and its anti-inflammatory activity. *Molecules* **2018**, *23*, 1258. [[CrossRef](#)]
35. Becerra, J.; Silva, M.; Delle-Monache, G.; Delle-Monache, F.; Botta, M. Two new chromenes from *Eupatorium glechonophyllum* Less. *Rev. Lat. Quím.* **1983**, *14*, 92–94.
36. Steinbeck, C.; Spitzer, V.; Starosta, M.; Poser, G. Identification of Two Chromenes from *Calea serrata* by Semiautomatic Structure Elucidation. *J. Nat. Prod.* **1997**, *60*, 627–628. [[CrossRef](#)]
37. Shamsuddin, K.M.; Musharraf, M.A.; Zobairi, M.O.; Ali, N. Demethylacetovanillochromene from *Tithonia diversifolia* (Hemes1.) A. Gray. *Indian J. Chem. Sect. B Org. Med. Chem.* **2001**, *8*, 751–752.
38. Zhai, H.L.; Zhao, G.J.; Yang, G.J.; Sun, H.; Yi, B.; Sun, L.N.; Chen, W.S.; Zheng, S.Q. A new chromene glycoside from *Tithonia diversifolia*. *Chem. Nat. Compd.* **2010**, *46*, 198–200. [[CrossRef](#)]
39. Bjeldanes, L.; Geissman, T. Euparinoid constituents of *Encelia californica*. *Phytochemistry* **1969**, *8*, 1293–1296. [[CrossRef](#)]
40. Bohlmann, F.; Zdero, C.; Franke, H. Naturally occurring coumarin derivatives. IX. Constituents of the genus *Gerbera*. *Chem. Ber.* **1973**, *106*, 382–387. [[CrossRef](#)]
41. Bohlmann, F.; Rao, N. New hydroxyacetophenone derivatives from *Espeletia schultzei*. *Chem. Ber.* **1973**, *106*, 3035–3038. [[CrossRef](#)]
42. Dupre, S.; Bohlmann, F.; Knox, E. Prenylated *p*-hydroxyacetophenone derivatives from the giant *Senecio johnstonii*. *Biochem. Syst. Ecol.* **1990**, *18*, 149–150. [[CrossRef](#)]
43. Achenbach, H.; Waibel, R.; Addae-Mensah, I. Constituents of West African medicinal plants. Part 17. Sesquiterpenes from *Carissa edulis*. *Phytochemistry* **1985**, *24*, 2325–2328. [[CrossRef](#)]
44. Schwartz, M.A. Syntheses of (+)- α - and (+)- β -eudesmol and their diastereomers by intramolecular nitron-olefin cycloaddition. *J. Org. Chem.* **1985**, *50*, 1359–1365. [[CrossRef](#)]
45. Castañeda, P.; Gómez, L.; Mata, R.; Lotina-Hennsen, B.; Anaya, A.L.; Bye, R. Phytochemical and Antifungal Constituents of *Helianthella quinquevenis*. *J. Nat. Prod.* **1996**, *59*, 323–326. [[CrossRef](#)]
46. Merfort, I.; Wendisch, D. Flavonoid glycosides from *Arnica montana* and *Arnica chamissonis*. *Planta Med.* **1987**, *53*, 434–437. [[CrossRef](#)] [[PubMed](#)]

47. Merfort, I.; Wendisch, D. New flavonoid glycosides from Arnicae flos DAB 91. *Planta Med.* **1992**, *58*, 355–357. [[CrossRef](#)] [[PubMed](#)]
48. Gutiérrez-Rebolledo, G.; Garduño-Siciliano, L.; García-Rodríguez, R.; Pérez-González, M.; Chávez, M.I.; Bah, M.; Siordia-Reyes, G.; Chamorro-Cevallos, G.; Jiménez-Arellano, M.A. Antiinflammatory and toxicological evaluation of *Moussonia deppeana* (Schldl. & Cham) Hanst and verbascoside as a main active metabolite. *J. Ethnopharmacol.* **2016**, *187*, 269–280.
49. Owona, B.A.; Njyouu, N.F.; Laufer, S.; Moundipa, P.F.; Schluesener, H.J. A fraction of stem bark extract of *Entada africana* suppresses lipopolysaccharide-induced inflammation in RAW 264.7 cells. *J. Ethnopharmacol.* **2013**, *149*, 162–168. [[CrossRef](#)]
50. An, X.; Gil, S.L.; Kang, H.; Heo, H.J.; Cho, Y.S.; Ok, D.M. Antioxidant and Anti-Inflammatory Effects of Various Cultivars of Kiwi Berry (*Actinidia arguta*) on Lipopolysaccharide-Stimulated RAW 264.7 Cells. *J. Microbiol. Biotechnol.* **2016**, *26*, 1367–1374. [[CrossRef](#)]
51. Lim, J.-Y.; Won, T.-J.; Hwang, B.-Y.; Kim, H.-R.; Hwang, K.-W.; Sul, D.; Park, S.-Y. The new diterpene isodojaponin D inhibited LPS-induced microglial activation through NF-kappaB and MAPK signaling pathways. *Eur. J. Pharmacol.* **2010**, *642*, 10–18. [[CrossRef](#)]
52. Hadi, G.; Ghanbari, R.; Delezar, A.; Nejad, E.S.; Yousef, M.M.; Bamdad, M.S.; Hamedayazdan, S.; Nazemiyeh, H. *Caccinia macrathera* Brand var. *macranthera*: Phytochemical analysis, phytotoxicity and antimicrobial investigations of essential oils with concomitant in silico molecular docking based on OPLS force-field. *Toxicol.* **2023**, *234*, 107291.
53. Merrill, G.B. Eupatoriochromene and enecalinal, plant growth regulators from yellow starthistle (*Centaurea solstitialis* L.). *J. Chem. Ecol.* **1989**, *15*, 2073–2087. [[CrossRef](#)]
54. Brito-Machado, D.; Ramos, Y.J.; Antunes, A.C.D.; Azevedo, G.Q.; Franklin, E.G.; Lima, M.D. Volatile chemical variation of essential oils and their correlation with insects, phenology, ontogeny and microclimate: *Piper mollicomum* Kunth, a case of study. *Plants* **2022**, *11*, 3535. [[CrossRef](#)] [[PubMed](#)]
55. Liu, X.-S.; Gao, B.; Dong, Z.-D.; Qiao, Z.-A.; Yan, M.; Han, W.-W.; Li, W.-H.; Han, L. Chemical compounds, antioxidant activities, and inhibitory activities against Xanthine oxidase of the essential oils from the three varieties of sunflower (*Helianthus annuus* L.) Receptacles. *Front. Nutr.* **2021**, *8*, 737157. [[CrossRef](#)] [[PubMed](#)]
56. Wright, C.; Chhetri, B.K.; Setzer, W.N. Chemical composition and phytotoxicity of the essential oil of *Encelia farinosa* growing in the Sonoran desert. *Am. J. Essent. Oil. Nat. Prod.* **2013**, *1*, 18–22.
57. Zeeshan, M.; Rizvi, S.M.D.; Khan, M.S.; Kumar, A. Isolation, partial purification and evaluation of bioactive compounds from leaves of *Ageratum houstonianum*. *EXCLI J.* **2012**, *11*, 78–88.
58. Yuan, Y.; Liub, Y.J.; Huang, L.Q.; Cuia, G.H.; Fua, G.F. Soil acidity elevates some phytohormone and β -eudesmol contents in roots of *Atractylodes lancea*. *Russ. J. Plant Physiol.* **2009**, *56*, 147–151. [[CrossRef](#)]
59. Yua, F.; Haradab, H.; Yamasakia, K.; Okamotoa, S.; Hirasec, S.; Tanakac, Y.; Norihiko, N.M.; Utsumia, R. Isolation and functional characterization of a β -eudesmol synthase, a new sesquiterpene synthase from *Zingiber zerumbet*. *FEBS Lett.* **2008**, *582*, 565–572. [[CrossRef](#)] [[PubMed](#)]
60. Britto, A.C.S.; de Oliveira, A.C.A.; Henriques, R.M.; Cardoso, G.M.B.; Bomfim, D.S.; Carvalho, A.A.; Moraes, M.O.; Pessoa, C.; Pinheiro, M.L.B.; Costa, E.V.; et al. In vitro and In Vivo antitumor effects of the Essential Oil from the leaves of *Guatteria friesiana*. *Planta Med.* **2012**, *78*, 409–414. [[CrossRef](#)]
61. Xue You, C.; Yang, K.; Fang, C.W.; Zhang, W.J.; Wang, Y.; Jiao, J.H.; Fan, L.; Shan, S.D.; Feng, Z.G.; Wei, Z.D. Cytotoxic Compounds Isolated from *Murraya tetramera* Huang. *Molecules* **2014**, *19*, 13225–13234. [[CrossRef](#)] [[PubMed](#)]
62. Ma, E.L.; Li, Y.C.; Tsuneki, H.; Xiao, J.F.; Xia, M.; Wang, M.W.; Kimura, I. β -Eudesmol suppresses tumor growth through inhibition of tumor neovascularization and tumor cell proliferation. *J. Asian Nat. Prod. Res.* **2008**, *10*, 159–167. [[CrossRef](#)]
63. Seo, M.J.; Kim, S.J.; Kang, T.H.; Rim, H.K.; Jeong, H.J.; Um, J.Y.; Hong, S.H.; Kim, H.M. The regulatory mechanism of β -eudesmol is through the suppression of caspase-1 activation in mast cell-mediated inflammatory response. *Immunopharmacol. Immunotoxicol.* **2011**, *33*, 178–185. [[CrossRef](#)]
64. Nam, S.Y.; Kim, H.Y.; Kim, H.M.; Jeong, H.J. Beta-eudesmol reduces stem cell factor-induced mast cell migration. *Int. Immunopharmacol.* **2017**, *48*, 1–7. [[CrossRef](#)]
65. Cinelli, M.A.; Do, H.T.; Miley, G.P.; Silverman, R.B. Inducible nitric oxide synthase: Regulation, structure, and inhibition. *Med. Res. Rev.* **2019**, *40*, 158–189. [[CrossRef](#)]
66. Hong, H.-J.; Loh, S.-H.; Yen, M.-H. Suppression of the development of hypertension by the inhibitor of inducible nitric oxide synthase. *Br. J. Pharmacol.* **2000**, *131*, 631–637. [[CrossRef](#)]
67. Möller, B.; Villiger, P.M. Inhibition of IL-1, IL-6, and TNF- α in immune-mediated inflammatory diseases. *Springer Semin. Immun.* **2006**, *27*, 391–408. [[CrossRef](#)] [[PubMed](#)]
68. Ding, C.; Cicuttini, F.; Li, J.; Jones, G. Target IL-6 in the treatment of inflammatory and autoimmune diseases. *Exper Opin. Investig. Drugs* **2009**, *18*, 1457–1466. [[CrossRef](#)] [[PubMed](#)]
69. Juergens, U.R. Anti-inflammatory properties of the monoterpene 1.8-cineole: Current evidence for co-medication in inflammatory airway diseases. *Drug Res.* **2014**, *64*, 638–646. [[CrossRef](#)] [[PubMed](#)]
70. Almeida, J.R.G.S.; Souza, G.R.; Silva, J.C.; Saraiva, S.R.G.D.; Junior, R.G.O.; Quintans, J.S.S.; Barreto, R.S.S.; Bonjardim, L.R.; Cavalcanti, S.C.H.; Junior, L.J.Q. Borneol, a bicyclic monoterpene alcohol, reduces nociceptive behavior and inflammatory response in mice. *Sci. World J.* **2013**, *2013*, 808460. [[CrossRef](#)] [[PubMed](#)]

71. Mankhong, S.; Iawsipo, P.; Srisook, E.; Srisook, K. 4-methoxycinnamyl *p*-coumarate isolated from *Etilingera pavieana* rhizomes inhibits inflammatory response via suppression of NF- κ B, Akt and AP-1 signaling in LPS-stimulated RAW 264.7 macrophages. *Phytomedicine* **2019**, *54*, 89–97. [[CrossRef](#)] [[PubMed](#)]
72. Wu, Y.L.; Han, F.; Luan, S.S.; Ai, R.; Zhang, P.; Li, H.; Chen, L.X. Triterpenoids from *Ganoderma lucidum* and Their Potential Anti-inflammatory Effect. *J. Agric. Food Chem.* **2019**, *67*, 5147–5158. [[CrossRef](#)]
73. Lyss, G.; Schmidt, T.J.; Merfort, I.; Pahl, H.L. **Helenalin**, an anti-inflammatory sesquiterpene lactone from Arnica, selectively inhibits transcription factor NF- κ B. *Biol. Chem.* **1997**, *378*, 951–961. [[CrossRef](#)]

Disclaimer/Publisher’s Note: The statements, opinions and data contained in all publications are solely those of the individual author(s) and contributor(s) and not of MDPI and/or the editor(s). MDPI and/or the editor(s) disclaim responsibility for any injury to people or property resulting from any ideas, methods, instructions or products referred to in the content.